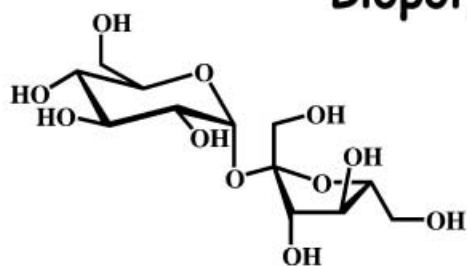
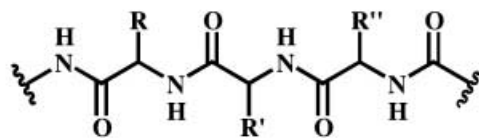


"Biopolymers of Life"

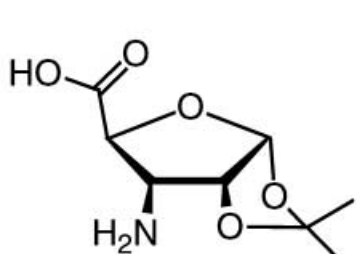


Carbohydrates

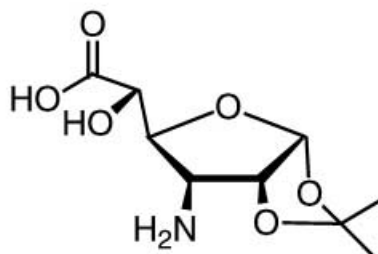


Peptides and Proteins

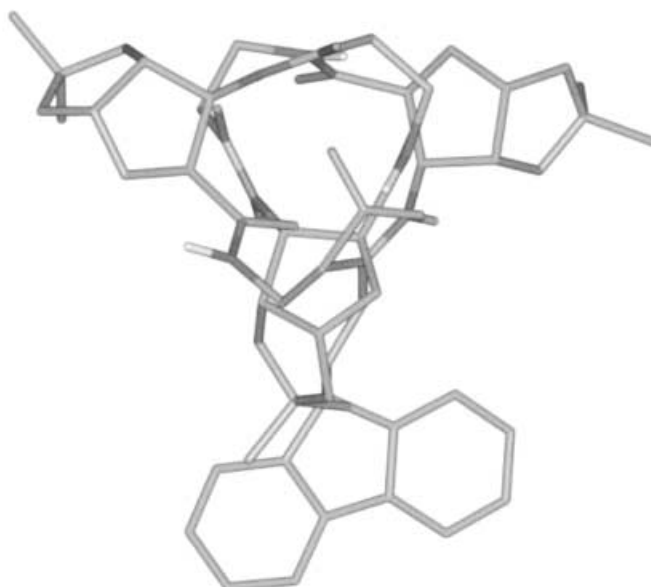
Sugar Amino Acids (SAA)



β -(Sugar) Amino Acid



γ -(Sugar) Amino Acid



Artificial Biopolymers with Predictable Solution Structures

Design, Synthesis, and NMR Structure of Linear and Cyclic Oligomers Containing Novel Furanoid Sugar Amino Acids

Sibylle A. W. Gruner,^[a, b] Vincent Truffault,^[b] Georg Voll,^[b] Elsa Locardi,^[b] Matthias Stöckle,^[b] and Horst Kessler^{*[a, b]}

Dedicated to Professor Dieter Seebach on the occasion of his 65th birthday

Abstract: Sugar Amino Acids (SAAs) are sugar moieties containing at least one amino and one carboxyl group. The straightforward synthesis of two furanoid SAAs, 3-amino-3-deoxy-1,2-isopropylidene- α -D-ribofuranic acid (f-SAA1) and 3-amino-3-deoxy-1,2-isopropylidene- α -D-allofuranic acid (f-SAA2) starting from diacetone glucose, is described. These SAAs were used as structural templates aiming at new structures for peptidomimetic drug design. f-SAA1 resembles a β -amino acid, whereas f-SAA2 is a γ -amino acid mimetic. Thus, for the synthesis of the mixed, linear and cyclic oligomers of f-SAA1, β -homoglycine (β -hGly, also called β -alanine) was chosen as an amino acid counter-

part, while for the oligomer of f-SAA2 γ -amino butyric acid (GABA) was chosen. Fmoc-[f-SAA1- β -hGly]₃-OH (**3**) and cyclo[f-SAA1- β -hGly]₃ (**5**) resemble linear and cyclic β -peptides with a very different substitution pattern, compared with the β -peptides known so far in the literature, whereas Fmoc-[f-SAA2-GABA]₃-OH (**4**) resembles a γ -peptide. The linear f-SAA oligomers **3** and **4** were synthesized on the solid-phase using Fmoc strategy. 23 unambiguous interresidue NOE contacts (from a total of 76

NOE values), obtained from extensive NMR studies in C₃CN, were used in subsequent simulated annealing and MD calculations, to elucidate the 12/10/12-helical structure of oligomer **3** in CH₃CN. The results indicate that f-SAA1 strongly induces a secondary structure. A characteristic CD curve for the linear oligomer **3** is observed up to 75 °C in both CH₃CN and CH₃CN/H₂O, even though **3** contains β -hGly, which is known to destabilize helices. By contrast, **4** does not seem to form a stable conformation in solution. The cyclic SAA containing oligomer cyclo[f-SAA1- β -hGly]₃ (**5**) exhibits a C₃ symmetric conformation on the NMR chemical shift time scale.

Keywords: amino acids • carbohydrates • conformation analysis • cyclopeptides • peptidomimetics

Introduction

Carbohydrates as well as peptides and proteins are essential biopolymers of life. They are involved in complex biological processes, such as catalysis and highly selective molecular recognition. In order to perform these functions, the correct folding of the biopolymers creating the active site is crucial, since any kind of interaction is observed only if the reactive groups are positioned in the correct spatial orientation. Thus, the development of small, easy-to-functionalize building

blocks and oligomers with backbones of discrete and predictable folding patterns ("foldamers")^[1] is required to design and develop molecules with biological functions. Therefore, chimeras of the three major classes of biopolymers, that is nucleic acids, proteins and carbohydrates, have attracted great interest as both functional and structural analogues in recent years, also because of their potential application in drug design. However, sugar amino acids (SAAs) and their oligomers, which bridge carbohydrates and proteins, have only recently been investigated.^[2–11]

We define SAAs as sugars, which contain at least one amino and at least one carboxyl group.^[2, 10, 11] Only few SAAs are found in nature,^[7, 11] the most prominent naturally occurring SAA being neuraminic acid, which constitutes the bacterial cell wall. This SAA and others served as templates for the earliest syntheses of SAAs by Heyns and Paulsen^[12] and Fuchs and Lehmann^[13] to mimic oligosaccharide structures, which remains the focus of most of the current SAA oligomer syntheses. Recently, we introduced SAAs as peptidomimetic structural templates (e.g. turn mimics),^[10, 11] to combine

[a] Prof. Dr. H. Kessler, Dr. S. A. W. Gruner
Novaspin Biotech GmbH, Lise-Meitner-Strasse 30
85354 Freising (Germany)
E-mail: kessler@ch.tum.de

[b] Prof. Dr. H. Kessler, Dr. S. A. W. Gruner, Dr. V. Truffault,
G. Voll, E. Locardi, M. Stöckle
Institut für Organische Chemie und Biochemie II
Technische Universität München
Lichtenbergstrasse 4, 85747 Garching (Germany)
Fax: (+49) 89 289 13210

polyfunctional carbohydrates with the amide backbone of peptides.^[2, 3]

The amide bonds between SAAs are formed in solution or on solid-phase using state-of-the-art peptide synthesis protocols. Thus, SAAs are ideal candidates for the generation of structural and functional combinatorial libraries. Their oligomers are potential structural templates of linear and cyclic peptides and pharmacophores. Nevertheless, their structural properties have to be scrutinized for a successful application.

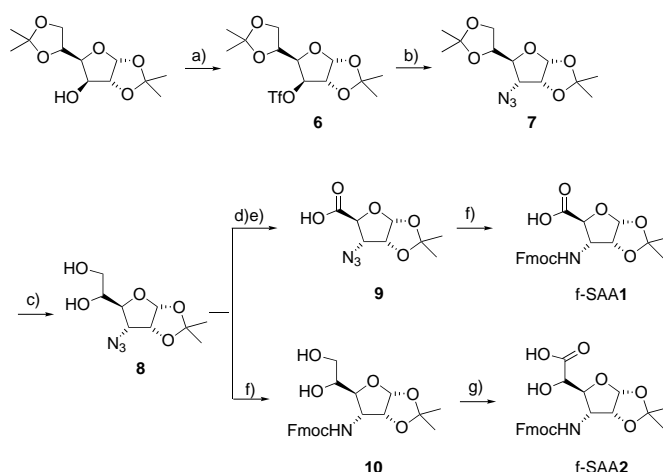
Pioneering work by Seebach's and Gellman's groups has revealed that short β - and γ -peptides form stable secondary structures such as helical, β -sheet type, and turn structures in both organic and aqueous solutions.^[1, 14–24] As for natural peptides, a correlation between characteristic circular dichroism (CD) curves and secondary structure of β - and γ -peptides was also demonstrated by the groups of Seebach and Gellman.^[15, 17, 19, 21, 22, 25–28]

Only few examples of mixed oligomers have been described so far. One example are mixed oligomers of a pyranoid SAA and aspartic acid, which was used as a β -amino acid. These compounds have been shown to inhibit cell adhesion of vitronectin binding cells and the invasion of tumor cells.^[29] Mixed oligomers consisting of SAAs and α -amino acids have only recently been described by our group^[30] and those of van Boom.^[31]

Results and Discussion

In this work, two new furanoid β - and γ -SAA building blocks will be presented as analogues of β - and γ -peptides, as structural templates, and as potential foldamers.^[32, 33] The linear mixed oligomer **3** and the cyclic mixed oligomer **5** consist of f-SAA1 and β -hGly (see footnote [a] Table 1; also β -alanine), thus forming hybrids between β -peptides. The linear mixed γ -hexapeptide **4** is built from alternating f-SAA **2** and γ -amino butyric acid (GABA) units. β -hGly and GABA were used as amino acid counterparts, because they represent, just as f-SAA1 and f-SAA2, β - and γ -amino acids, respectively. Since the amino acids are completely unsubstituted, the secondary structure results exclusively from the incorporated SAA.

Synthesis of the f-SAA1 and 2: The synthesis of f-SAA1 has already been described in the preliminary communication.^[36] The syntheses of furanoid f-SAA1^[36] and f-SAA2 are shown in Scheme 1. Both were synthesized via the azides **7** and **8**. The crucial step is the azidolysis of trityl-activated diacetone glucose **6**. The major elimination side reaction, which results from the poor solubility of azides in organic solvents, has been known in the literature.^[37–39] We were able to obtain considerably higher yields than in ref. [37] (70 % instead of 48 %) by the addition of catalytic amounts of the phase transfer catalyst Bu₄NCl, at the same time avoiding expensive^[39] and/or toxic^[38] reagents. This reagent significantly increases the solubility of NaN₃. Thus, triflate-ester **6** was converted at 50 °C in DMF to the azide **7** in 70 % yield with inversion of configuration at the C³ center. Efforts to further enhance



Scheme 1. Synthesis of Fmoc-protected f-SAA1 and **2**: a) Tf₂O, py, –10 °C, CH₂Cl₂; b) NaN₃, Bu₄NCl (cat), 50 °C, DMF; c) 77 % HOAc, 3 h, 65 °C; d) NaIO₄, 5 h, 10 °C, MeOH; e) KMnO₄, 50 % HOAc, rt; f) H₂, Pd/C, MeOH, Fmoc-Cl, NaHCO₃, pH 8–9, THF, MeOH, rt, 90 %; g) NaOCl, TEMPO (cat), KBr, CH₂Cl₂, sat. aq. NaHCO₃, Bu₄NCl, 62 %.

substitution yields and suppress elimination more efficiently by using the “naked” azide-anion generated in situ from trimethylsilylazide and *t*Bu₄NF failed: Only elimination was observed and **7** could not be detected.

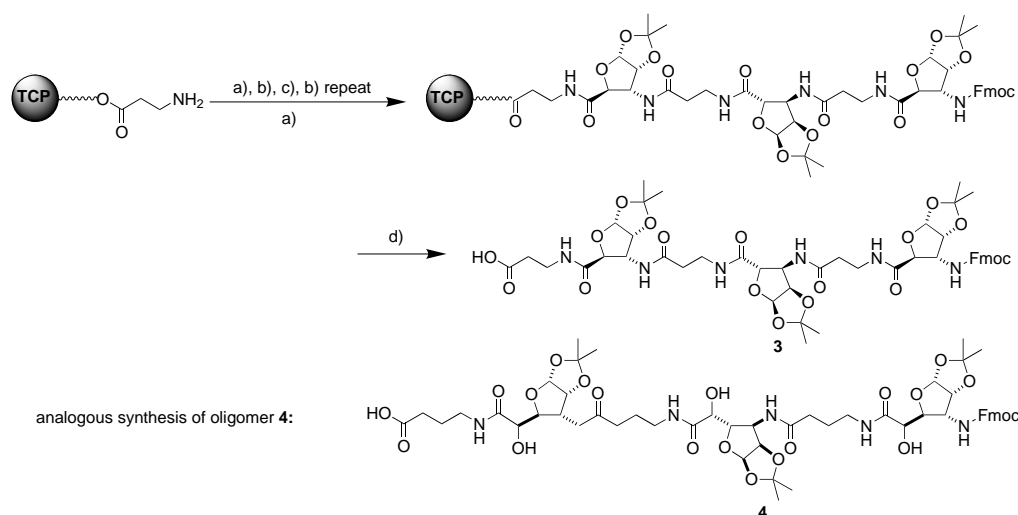
Azidolysis was followed by quantitative deprotection of the exocyclic hydroxyl groups using acetic acid.^[40] To obtain Fmoc-protected f-SAA1, diol **8** was cleaved oxidatively using NaIO₄, followed by KMnO₄ oxidation to yield **9**.^[40] In a one-pot reaction, azide **9** was reduced and simultaneously Fmoc-protected to yield about 70 % of Fmoc-protected f-SAA1.

For the preparation of f-SAA2, azide **8** was first reduced and Fmoc-protected in a similar one-pot reaction as for **9**, followed by selective oxidation of the primary alcohol with 2,2,6,6-tetramethylpiperidin-1-oxyl (TEMPO), sodium hypochlorite, and KBr. To prevent decarboxylation during the TEMPO oxidation, it was crucial to keep the pH between 8.5 and 9.5, and the temperature below 0 °C.

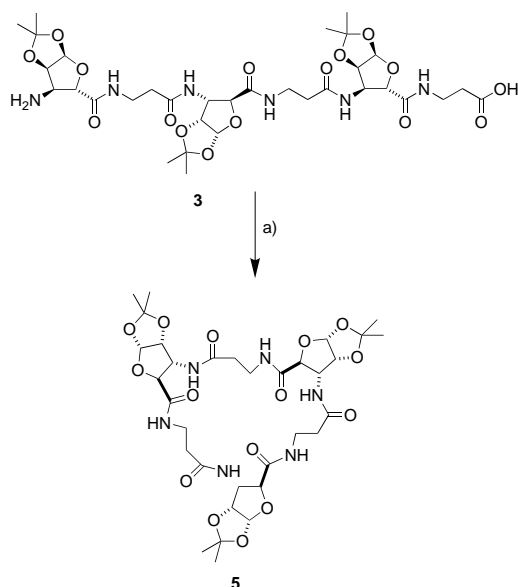
Synthesis of the oligomers 3, 4 and 5: The mixed SAA oligomers **3** and **4** were synthesized as shown in Scheme 2. f-SAA1 and f-SAA2 were alternately coupled with β -homoglycine or GABA to form oligomers **3** and **4**.

The solid-phase synthesis was performed on the tritylchloropolystyrene (TCP) resin using [*O*-(7-azabenzotriazol-1-yl)-1,1,3,3-tetramethyluronium hexafluorophosphate] (HATU) as the coupling reagent and 2,4,6-collidine as the base.^[41–43] Two equivalents of the SAA derivative, and three equivalents of β -homoglycine or GABA were employed. After the peptide was cleaved from the resin with hexafluoroisopropanol (20 % in dichloromethane, 3 × 10 min),^[44] RP-HPLC purification yielded the oligomer **3** (71.3 mg, 41 % yield) and **4** (10 mg, 4.7 % yield), each in over 99 % HPLC purity.

Subsequently the Fmoc group was then removed and the linear oligomer **3** cyclized with HATU/2,4,6-collidine at high dilution (0.4 mM) to afford **5** in quantitative yield (Scheme 3).



Scheme 2. Synthesis of the linear oligomer **3**: a) HATU (2 equiv), 2,4,6-collidine (20 equiv), f-SAA1 (2 equiv), rt, NMP; b) i) washing: NMP (5 × 3 min), ii) Fmoc deprotection: 20% piperidine in DMF (2 × 10 min), iii) washing: NMP (5 × 3 min); c) HATU (3 equiv), 2,4,6-collidine (30 equiv), β -hGly (3 equiv), rt, NMP; d) i) washing: NMP (3 × 3 min), CH_2Cl_2 (1 × 3 min), ii) vacuo overnight, iii) cleavage: 20% HFIP in CH_2Cl_2 (3 × 10 min).



Scheme 3. Cyclisation of the linear oligomer **3** to the cyclic **5**: a) Fmoc deprotection: 20% pip in DMF (2 × 10 min); b) cyclization in DMF (0.45 mM), HATU (1.1 equiv), 2,4,6-collidine (11 equiv).

CD spectroscopic analysis: The secondary structure of peptides and proteins consisting of α -amino acids in solution can be deduced by CD spectroscopy. Recently, the Gellman and Seebach groups expanded the use of CD spectroscopy to prove the secondary structure of β - and γ -peptides,^[15, 17, 19, 21–23, 25–28] different secondary structure elements can be identified by characteristic CD curves.

The CD data for **3** in CH_3CN and $\text{CH}_3\text{CN}/\text{water}$ solutions at various temperatures (Figure 1) reveal a distinctive secondary structure of this linear oligomer. In order to allow comparison of the different CD curves of the mixed oligomers **3–5** and monomeric f-SAA1 and f-SAA2, we divided each curve by the number of amide bonds present. Comparison of the CD curves of the Fmoc-protected f-SAA1 with the curves of the linear mixed oligomer **3** (Figure 1a) shows, that the major

part of the observed molar ellipticity θ per residue is a result of cooperative effects due to the orientation of the backbone amide chromophores, and not a result of a single chromophore within the f-SAA1 residues. The CD spectrum of **3** (Figure 1a) comprises a strong minimum at about 188 nm, a zero crossing at about 193 nm, and a strong maximum at about 203 nm. It is different from the CD spectrum of any β -peptide so far known. However, the contribution of the substitution pattern and chiral centers within the side chain to the observed molar ellipticity θ has never been determined. Therefore, the known β -peptide structures can not be excluded.

As expected for secondary structural effects, the maxima of the CD curves decrease with increasing temperature (Figure 1b). A random structure would show the same average spectrum at all temperatures. When changing the solvent from the relatively unpolar solvent CH_3CN to a 1:1 mixture of CH_3CN and water, the molar ellipticity of **3** decreases to almost half of the value in pure CH_3CN (Figure 1c). This may be due to the fact that the secondary structure, to which the curve corresponds to, is less stable in more polar solvents. As the CD profile of **3** in CH_3CN and $\text{CH}_3\text{CN}/\text{water}$ solutions at temperatures between 20 and 75 °C is independent of the concentration between 0.125 and 1 mM, it seems unlikely that aggregation occurs under these conditions.

The typical CD signature of **3** is lost upon cyclization to **5** (Figure 1d). This implies a drastic change of the orientation of the backbone amide chromophores upon cyclization.

Due to the low solubility of **4** in CH_3CN , no CD spectra were recorded in this solvent. The CD spectra of **4** in MeOH did not provide any useful structural information, because the spectra were not very intense, and almost temperature independent. This suggests that there is no stable secondary structure of **4** in MeOH.

NMR- and structural analysis: Two-dimensional NMR data were obtained for **3** (10 mM) in CD_3CN at 300 K. All ^1H NMR resonances of each of residue spin systems were assigned by

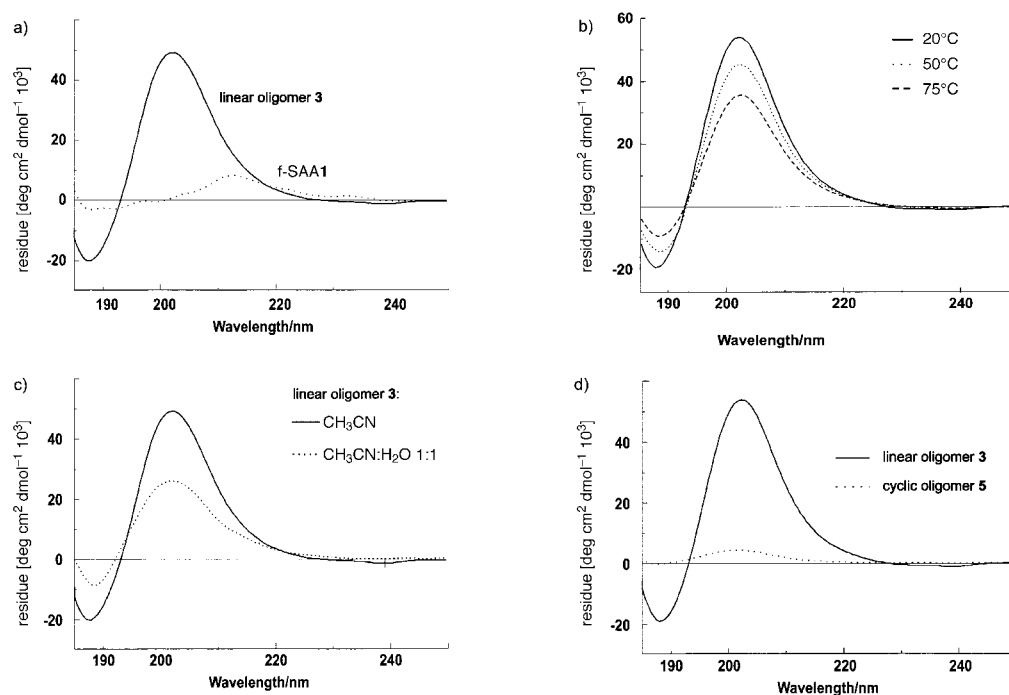


Figure 1. a) CD spectra (molar ellipticity Θ per residue in $\text{deg cm}^2 \text{dmol}^{-1} \cdot 10^3$) of the linear Fmoc-[f-SAA1- β -hGly]₃-OH (**3**) and Fmoc-f-SAA1-OH in CH₃CN at 20 °C at 0.125 mM (**3**), and 0.5 mM (**1**). b) CD data for the linear Fmoc-[f-SAA1- β -hGly]₃-OH (**3**) at 0.125 mM in CH₃CN at 20, 50 and 75 °C. c) CD data for the linear Fmoc-[f-SAA1- β -hGly]₃-OH (**3**) at 0.125 mM in CH₃CN and CH₃CN/water (1:1). d) CD spectra of the linear Fmoc-[f-SAA1- β -hGly]₃-OH (**3**) and its cyclic analogue cyclo-[f-SAA1- β -hGly]₃ (**5**) at 0.125 mM and 20 °C in CH₃CN.

means of TOCSY^[45] and COSY spectra.^[46] The assignment of backbone resonances was accomplished using sequential C_β , C' , H^α and H^N chemical shift information derived from HMQC^[47] and HMBC^[48] experiments as outlined in the Experimental Section. All carbon chemical shifts were assigned, except for the quarternary Fmoc carbon atoms, the quarternary carbons of the acetamide protecting groups of the SAAs, and the terminal carbon of the carboxylate function. Stereospecific assignment, made under the consideration of the NOESY^[49] cross-peak patterns, was possible for all prochiral H^α and H^β protons of the β -homoglycine residues and for the prochiral methyl groups of all f-SAA1 residues, except for the terminal H^α and H^β resonances of β -hGly **6**.

The secondary structure of **3** in CD₃CN is defined by 23 interresidue NOE contacts (see Experimental Section Table 2) and a total set of 76 NOE restraints deduced from a NOESY experiment.

A first restrained conformational search, based on these 76 NOE cross-peaks, was performed by utilizing standard simulated annealing protocols with the X-PLOR package,^[50] yielding an ensemble of 10 structures with good convergence. The structure which best fulfilled the experimental restraints was then used as a starting structure for a 150 ps simulated dynamics run with the Discover program package,^[51] utilizing its CVFF forcefield for further refinement. The refinement was performed in an explicit, all-atom CH₃CN solvent box which we have developed for this purpose (for details see Experimental Section). This yielded the averaged structure of **3** depicted in Figure 2. The averaged structure was finally used as a starting structure for a further unrestrained dynamics simulation, and remained stable in the CVFF forcefield.

The conformation deduced is right-handed helical, with the helix consisting of a central 10-membered and two terminal 12-membered hydrogen-bond rings, and with C=O and N-H bonds pointing alternatively up and down along the axis of the helix. Four hydrogen bonds are formed, which are shown schematically in Figure 3.

We have carefully checked for evidence of all other possible helix types, which β -peptides may adopt as predicted by quantum mechanical calculations.^[52–54] All distinctive cross-peaks for the other possible helix types 10/10/10, 12/12/12, and 14/14/14, as well as for the most likely 10/12/10 helix (the counterpart of the observed 12/10/12 helix), were missing in the NOESY spectrum. All other characteristic distances, which would lead to strong signals for the mentioned helices, are represented by only weak signals in the spectrum. We therefore conclude that **3** adopts a plain 12/10/12 helical conformation in CH₃CN in competition with a slightly unfolded helix (see Experimental Section).

This is the first time that this type of helix was found for SAA-homooligomers or short SAA- β -amino acid conjugates. So far, a similar helix has only been found by Seebach and co-workers for β -peptides with side chains identical to those of the naturally occurring α -amino acids.^[25, 55] The substitution pattern of β -peptides, which have been shown to form this “mixed 12/10/12 helix”, is very different from that of **3**. Oligomer **3** (when considered a β -peptide) consists of alternating (*S,S*)-disubstituted β -(sugar) amino acid (here, only the substitution along the resulting peptidic backbone is considered) and unsubstituted β -hGly, denoted [*S,S*-U]₃, according to the nomenclature of Hofmann and co-workers^[53] (see Table 1). Seebach's β -peptide, however, shows a very different

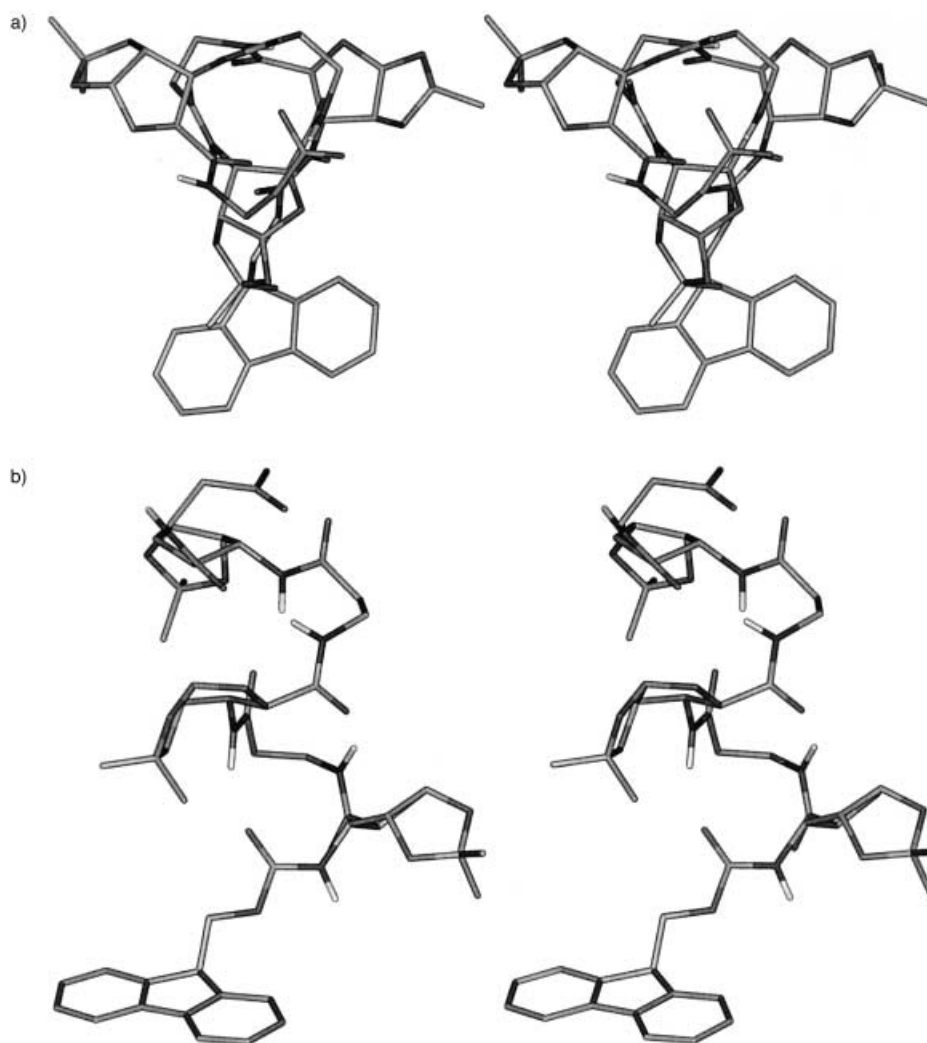


Figure 2. Stereoview of the average structure of oligomer **3**, as deduced by a 150 ps restrained molecular dynamics simulation in an explicit, all-atom CH₃CN solvent box. Top view a) and side view b) of the formed right handed 12/10/12-helix of **3**, consisting of a central 10-membered and two terminal 12-membered H-bonded rings, and with C=O and N-H bonds pointing alternately up and down along the axis of the helix are shown.

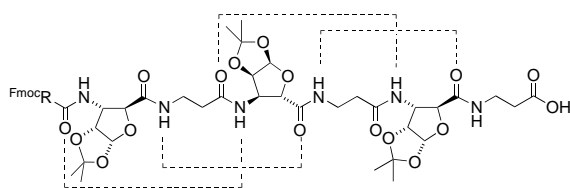


Figure 3. Schematic drawing of hydrogen bonds formed in the CH₃CN solution structure of oligomer **3**.

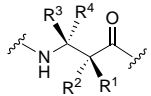
substitution pattern of [BA]₃, where the β -amino acid residues are alternately (*S*)-monosubstituted in the α - or in the β -position.

The quantum-mechanical investigation of β -peptides by Hofmann and co-workers^[52] reveals that helix types 10/10/10, 12/12/12, 14/14/14, 10/12/10 and 12/10/12 are stable conformations for various types of β -peptides (either with one or two different amino acids in the repeat unit); the most stable conformation depends on the substitution pattern of the amino acid. Interestingly, for an alternating [BA] substitution pattern, helix type 12/10/12 is predicted to be the most stable

type in non-polar solvents. This may be ascribed to the fact that the carbonyl functions point alternately towards the N-terminus and the C-terminus in the 12/10/12-helix; this results in a low overall dipole momentum of the helix. For the [BA]-substitution pattern, the spatial constraints imposed by the β -substituent of the first amino acid in the sequence leads to a lower energy of the helix 12/10/12 with respect to the helix 10/12/10, which also has a low overall dipole momentum. Furthermore, it has been shown that substitution in β -position has a considerably higher structural influence than substitution in α -position.^[54] Therefore, the influence of the β -substituent will dominate over that of the α -substituent in a [*S,S*]-substituted β -amino acid. On the other hand, an unsubstituted β -amino acid lacks a β -substituent with strong structural influence. Thus, the structural influence of the [*S,S*]-substituted f-SAA1 in **3** is rather similar to a [B]-substituted β -amino acid compared with an [A]-substituted one. The characteristic feature of [A]-substituted β -amino acids is the lack of substitution in the β -position. Therefore the overall unsubstituted β -hGly in **3** acts like an [A]-substituted β -

amino acid. As a consequence, the substitution pattern of [*S,S,U*]₃ in oligomer **3** should induce similar secondary structures as the [AB]₃ substitution pattern of Seebach's "mixed" β -peptides. This would explain why oligomer **3** forms the 12/10/12-helical structure in CD₃CN.

Table 1. Nomenclature of substitution patterns of β -peptides.

					
R ¹	R ²	R ³	R ⁴	Seebach ^[a]	Symbol
H	H	H	H	- β -hGly-	-U-
R \neq H	H	H	H	-(<i>S</i>) β^2 -hXaa-	-A-
H	H	R \neq H	H	-(<i>S</i>) β^3 -hXaa-	-B-
H	R \neq H	R \neq H	H	-(<i>R,S</i>) $\beta^{2,3}$ -hXaa-	- <i>R,S</i> -
R \neq H	H	R \neq H	H	-(<i>S,S</i>) $\beta^{2,3}$ -hXaa-	- <i>S,S</i> -

[a] The notation β -hXaa for a homologue of the α -amino acid Xaa was introduced by Ondetti and co-workers,^[34] and has been used and refined by Seebach and co-workers to β^2 - and β^3 -hXaa, where the numbers indicate the position of the side chains in the β -amino acids.^[35]

NMR structural analysis of oligomer **3** in DMSO revealed, that a 12/10/12 helix is no longer formed exclusively. This observation is in agreement with the CD-spectroscopic results and quantum mechanical calculations, which reveal, that helices with a permanent large dipole moment is favored in polar solvents over helices with a small dipole moment (such as the 12/10/12 helix).^[52–54] However, large J coupling constants of about 9 Hz were observed between the H^N of its f-SAA1 residues and their H^3 (the “H a ”). The dihedral H^N/H^3 angle should be mainly *trans*. The conformation of the f-SAA1 residues in the linear oligomer **3** in DMSO was deduced with the refined Karplus equation by Haasnoot et al.^[56] utilizing the coupling constants $^3J(H^1, H^2)$ of 5.3 Hz, $^3J(H^3, H^4)$ of 10 Hz, and $^3J(H^N, H^3)$ of 8.9 Hz of the f-SAA1 residues. In their equation,^[56] the relationship between vicinal NMR proton–proton coupling constants and the pseudorotational properties of the furanoid sugar ring are taken into account, which allows an accurate correction for the effects of electronegativity and orientation of substituents on $^3J(H, H)$.^[56] The H^N chemical shifts are also still well dispersed. Therefore, **3** must form some kind of ordered structure. However, due to large overlaps of the sugar and alkyl protons in the NOESY spectra (in DMSO), the integration of several cross-peaks is not possible, thus preventing reliable three-dimensional structure modeling.

NMR studies of **4** and **5** at 500 or 600 MHz in DMSO and/or pyridine were performed. Full sequential assignment of **4** and **5** was achieved similar to the above described procedure for **3**. NOESY and ROESY spectra were recorded to obtain three-dimensional structural information. The amide protons of the linear oligomers **4** have different chemical shifts, however, due to large overlap of several NOE signals, no reliable structure calculation is possible.

The cyclic oligomer **5** exhibits apparent C_3 symmetry on the NMR chemical shift time scale, and averaged J -coupling constants of 7 Hz between the H^N and the H^3 protons of the f-SAA1 residues in DMSO.

Conclusion

The straightforward syntheses of two new furanoid sugar amino acids, in a few steps from diacetone glucose, are described. This makes them easily accessible and therefore useful building blocks for combinatorial syntheses. f-SAA1 resembles a β -amino acid, while f-SAA2 resembles a γ -amino acid. Thus, f-SAA1 was used with β -homoglycine for the synthesis of the linear and cyclic mixed oligomers **3** and **5**. For the synthesis of linear oligomer **4**, f-SAA2 was used with GABA as an amino acid counterpart. Oligomers **3** and **4** were assembled successfully using standard solid-phase peptide synthesis. To the best of our knowledge, the mixed oligomers **3**, **4** and **5** presented here are the first conjugates of furanoid sugar amino acids with β - and γ -amino acids.

The linear Fmoc-[f-SAA1- β -hGly]₃-OH (**3**) exhibited 12/10/12 helical secondary structure in CH₃CN and CH₃CN/H₂O solutions as proven by NMR studies and subsequent molecular dynamics calculations. This is significant, since **3** has a very different substitution pattern than the β -peptides so far

shown to have a secondary structure. Furthermore, **3** contains β -homoglycine, which is known to destabilize helices.^[57] Stable secondary structures were so far only reported for β -peptides consisting almost exclusively of α - or β -substituted β -amino acids. It is obvious that the unsubstituted β -homoglycine is much more flexible (compare Gly substitution of L- α -amino acids in α -peptides). Hence, f-SAA1 strongly induces the secondary structural element of a 12/10/12-helix in short oligomeric sequences. However, the 12/10/12 preferred helical conformation is lost in polar DMSO. The more flexible Fmoc-[f-SAA2-GABA]₃-OH (**4**) shows random coil behaviour.

Another remarkable feature is the good solubility of cyclo-[f-SAA1- β -hGly]₃ (**5**) in organic solvents, such as CH₃CN, DMSO and MeOH. Cyclic β -peptides prepared by Seebach et al. exhibited low solubility in classical, pure organic solvents.^[15, 58–59] Thus, one-dimensional NMR studies were either not possible, or [D₈]THF solutions with more than ten equivalents of anhydrous LiCl had to be used.^[59] Cyclic oligomer **5** exhibits a C_3 symmetric conformation on the NMR chemical shift time scale. However, our preliminary NMR results do not yet give evidence of a clearly distinct conformation, since the observed NMR signals are averaged and similar to those of the monomeric subunits.

The new compounds presented here are useful as new structural templates^[11, 36] and might also be of interest for host–guest chemistry.^[31, 60]

Experimental Section

General: Solvents for moisture sensitive reactions were distilled and dried according to standard procedures. All other solvents were distilled before use. Pd/C was donated by Degussa, Frankfurt/M. (Germany). Flash column chromatography (FC) was performed with solvents indicated on silica gel 60, 230–400 mesh (Merck KGaA, Darmstadt). For solid-phase synthesis TCP resin (tritylchloropolystyrene resin) from PepChem Goldammer & Clausen, H- β -hGly-2-ClTrt resin and Fmoc- β -hGly-OH from Novabiochem, HATU from Perseptive Biosystems and Fmoc-GABA-OH (Fmoc-4-aminobutyric acid) from Neosystems were used. All reactions were monitored by thin-layer chromatography with 0.25 mm precoated silica gel 60 F₂₅₄ aluminium plates (Merck KGaA, Darmstadt). Melting points were obtained on a Büchi-Tottoli apparatus and are uncorrected. RP-HPLC analysis and semiscale preparations were carried out on a Waters (high pressure pump 510, multi-wavelength detector 490E, chromatography workstation Maxima 820), a Beckman (high pressure pump 110B, gradient mixer, controller 420, UV detector Uvicord from Knauer), or an Amersham Pharmacia Biotech (Äkta Basic 10/100, autosampler A-900) facility. RP-HPLC preparative separations were carried out on a Beckman System Gold (high pressure pump module 126, UV detector 166). C₁₈ columns were used. As solvents, solvent A: H₂O + 0.1% CF₃COOH, and B: CH₃CN + 0.1% CF₃COOH with UV detection at 220 and 254 nm, were used. ¹H, and ¹³C, and 2D NMR spectra were recorded on either Bruker AC250, DMX500 or DMX-600 spectrometers. Proton chemical shifts are reported in ppm relative to residual CHCl₃ (δ =7.24), DMSO (δ =2.49) or pyridine (δ =7.19, 7.55, 8.71). Multiplicities are given (obtained from 1D spectra) as s (singlet), d (doublet), t (triplet), q (quartet), m (multiplet), br (broad). ¹³C chemical shifts are reported relative to CDCl₃ (δ =77.0), [D₆]DMSO (δ =39.5) and [D₅]pyridine (δ =123.5, 135.5, 149.9). Data was processed on a Bruker X32 workstation using the UXNMR-software. Assignment of proton and carbon signals was achieved by HMQC,^[47] COSY,^[46] TOCSY^[45] and HMBC^[48] experiments. Coupling constants were determined whenever possible from the corresponding 1D spectrum, and in some cases from different COSY experiments. HPLC-ESI mass spectra were recorded on a Finnigan NCQ-ESI with HPLC conjunction LCQ (HPLC-system Hewlett

Packard HP 1100, Nucleosil 100 5C₁₈). IR spectra were recorded on a Perkin–Elmer 257 spectrophotometer. High-resolution mass spectra were performed by the Department of Chemistry of the Ludwigs Maximilians University of Munich on Finnigan MAT 95Q using fast ion bombardment with Cs⁺ ions and *m*-nitrobenzylalcohol (matrix).

General procedure for reduction and simultaneous Fmoc protection of azides (GP 1): A stirred solution of the azide in MeOH/H₂O 2:1 (0.15 M) is adjusted to pH 8 with saturated NaHCO₃ solution. A solution of Fmoc-Cl (1.1 equiv) in THF (0.16 M) is added to this solution, followed by the addition of the catalyst Pd/C (Degussa E101 w/w 10%, wet 49.7% H₂O, 1 g cat per g azide). The suspension is flushed several times with H₂. The reaction is generally completed after 18–24 h (TLC control). Solvents are removed under reduced pressure. The residue is suspended in water, and the pH is adjusted to 8–9 with saturated NaHCO₃ solution, and the aqueous phase is extracted with AcOEt (3 ×). The combined organic phases are washed with NaHCO₃. The aqueous phase is adjusted to pH 1 with 1 N HCl and extracted with AcOEt (3 ×). The organic phase is washed with sat. aqueous NaCl solution, dried (MgSO₄) and concentrated under reduced pressure.

General procedure for solid-phase synthesis of the oligomers 3 and 4 (GP 2): The Fmoc-protecting group of the amino acid attached to the resin is removed by treating the resin with a 20% piperidine solution in DMF (2 × 10 min). The resin is filtered off and washed with NMP (5 × 3 min), before a solution of the next Fmoc-protected amino acid (2 equiv Fmoc-SAA-OH, 3 equiv Fmoc-β-hGly-OH or Fmoc-GABA-OH), HATU (2 equiv for SAA coupling, 3 equiv for other amino acids), and 2,4,6-collidine (20 equiv/30 equiv) in NMP is added. After 3–48 h reaction is complete (monitoring by ESI-HPLC-MS). The resin is washed with NMP (5 × 3 min), prior to the subsequent Fmoc deprotection and coupling steps. After coupling of the last amino acid, the resin is washed with NMP (3 × 3 min), CH₂Cl₂ (1 × 3 min), and dried overnight under vacuo. The oligomers are cleaved from the dry resin using 20% HFIP solution in CH₂Cl₂ (3 × 10 min). The crude peptides were purified by RP-HPLC.

1,2,5,6-Di-*O*-isopropylidene-3-*O*-triflyl-α-D-glucufuranose (6): Triflic anhydride (54.2 g, 0.192 mol) was slowly added to a stirred solution of diacetone glucose (25 g, 0.96 mol), and pyridine (30.39 g, 0.384 mol) in CH₂Cl₂ (1 L) in a three-necked flask at –10 °C (acetone/ice bath).^[61, 62] Pyridinium triflate salt precipitated, and the solution turned brown. The reaction was complete after 1.5 h (TLC control: AcOEt/hexane 2:1). The reaction mixture was poured onto ice water (1 L). The aq phase was extracted with CH₂Cl₂ (4 ×). The organic phases were dried (MgSO₄), and repeatedly coevaporated with toluene to remove pyridine. The brown residue was extracted with hexane (3 ×). Evaporation of hexane yielded the desired product as white crystals (36.88 g, 98%). *R*_f = 0.61 (AcOEt/hexane 2:1); m.p. and ¹H NMR were in agreement with ref. [62]

3-Azido-3-deoxy-1,2,5,6-di-*O*-isopropylidene-α-D-allofuranose (7): A solution of the above described triflyl sugar (37.1 g, 0.0945 mol) in DMF (200 mL) was added slowly to a solution of NaN₃ (12.3 g, 0.189 mol), Bu₄NCl (catalytic, ≈0.1 g) in DMF (1.5 L) at 50 °C. The reaction was complete after 5 h of stirring at 50 °C (TLC control: AcOEt/hexane 2:1). DMF was removed under reduced pressure, and the residue was dissolved in AcOEt. The organic phase was washed with H₂O (2 ×). The aqueous phase was re-extracted with AcOEt (2 ×) until TLC showed no traces of **7**. The combined organic phases were dried (MgSO₄) and evaporated to yield a syrup of crude **7** and elimination by-product. (¹H NMR gave a ratio of **7** to elimination product of 7:3). The crude product **7** was purified by FC (AcOEt/hexane 1:3) to yield **7** (18.2 g, 70%) as a colorless liquid. *R*_f = 0.55 (AcOEt/hexane 1:3); ¹H NMR of both **7** and of the elimination product were in agreement with ref. [39].

3-Azido-3-deoxy-1,2-*O*-isopropylidene-α-D-allofuranose (8): For the oxidation,^[40] **8** (16 g, 0.056 mol) was dissolved in AcOH (77%, 38 mL) and stirred under reflux for 3 h. After evaporation of the organic solvent, crude **8** was purified by FC (AcOEt/hexane 2:1) to give **8** as white crystals (12.9 g, 94%). M.p. and ¹H NMR were in agreement with ref. [63].

3-Azido-3-deoxy-1,2-*O*-isopropylidene-α-D-ribofuranose aldehyde: NaIO₄ (8.4 g, 0.036 mmol) was added gradually to a cooled solution (10 °C) of **8** (8 g, 0.0327 mol) in MeOH (60 mL) and H₂O (100 mL).^[40] The mixture was stirred for 5 h. The inorganic salts were precipitated by the addition of MeOH (150 mL), filtered off, and washed several times with MeOH. The combined organic phases were removed under vacuum to yield the

aldehyde as a light yellow syrup. The crude aldehyde was used without further purification for the oxidation to **9**. ¹H NMR (250 MHz, CDCl₃/MeOD, 298 K): δ = 1.35 (s, CH₃), 1.55 (s, CH₃), 3.65 (dd, *J*_{3,4} = 4.72, *J*_{2,3} = 4.37 Hz, H³), 4.1 (d, *J* = 4.7 Hz, H⁴), 4.7 (dd, *J*_{1,2} = 3.7, *J*_{2,3} = 4.5 Hz, H²), 5.9 (d, *J*_{1,2} = 3.8 Hz, H¹), 9.7 (brs, H⁵).

3-Azido-3-deoxy-1,2-*O*-isopropylidene-α-D-ribofuranic acid (9): KMnO₄ (6.7 g, 42 mmol) was added slowly to a stirred solution of the above described aldehyde in HOAc (50%, 150 mL) resulting in a purple solution.^[40] After 12 h reaction was complete. The solution was adjusted to pH 1 with conc. HCl, excess KMnO₄ was removed with Na₂SO₃. The solution was extracted with CHCl₃ (3 ×). The organic phase was dried (MgSO₄) and concentrated under reduced pressure. Recrystallization from AcOEt/hexane afforded **9** (4.29 g, 1.87 mmol, 89% over two steps) as white crystals.

3-Amino-3-deoxy-*N*-9-fluorenylmethoxycarbonyl-1,2-isopropylidene-α-D-ribofuranic acid (f-SAA1): According to GP 1, azide **9** (1 g, 4.36 mmol) was reduced to the amine and simultaneously Fmoc-protected to yield f-SAA1 (1.4 g, 3.29 mmol, 76%) as a colorless syrup which later crystallized. ¹H NMR (500 MHz, [D₆]DMSO, 300 K): δ = 1.26 (s, 3H, CH₃), 1.46 (s, 3H, CH₃), 4.07 (m, H³), 4.22 (m, 1H, Fmoc-CH), 4.25 (m, 1H, H⁴), 4.30 (m, 2H, CH₂^{Fmoc}), 4.60 (t, *J* = 4.0 Hz, 1H, H²), 5.84 (d, *J* = 3.4 Hz, 1H, H¹), 7.32 (m, H^{arom}), 7.40 (m, H^{arom}), 7.63 (m, H^N), 7.72 (m, H^{arom}), 7.87 (d, *J* = 7.3 Hz, 2H, H^{arom}); ¹³C NMR (125 MHz, [D₆]DMSO, 300 K): δ = 26.06 (CH₃), 26.29 (CH₃), 46.30 (CH^{Fmoc}), 56.25 (C³), 65.61 (CH₂^{Fmoc}), 75.36 (C⁴), 78.01 (C²), 104.17 (C¹), 111.63 (C^{isoprop}), 119.75 (C^{arom}), 124.89 (C^{arom}), 127.17 (C^{arom}), 143.32 (C⁵); FAB-HRMS: calcd for C₂₃H₂₃NO₇Na: 448.1372; found: 448.1366 [*M*+Na]⁺.

3-Amino-3-deoxy-*N*-9-fluorenylmethoxycarbonyl-1,2-isopropylidene-α-D-allofuranose (10): According to GP 1, azide **8** (2 g, 8.31 mmol) was reduced to the amine and Fmoc-protected. FC (AcOEt/hexane 1:1 → 1) afforded **10** (3.3 g, 748 mmol, 92%) as a white powder. ¹H NMR (500 MHz, CDCl₃, 300 K): δ = 1.35 (s, 3H, CH₃), 1.55 (s, 3H, CH₃), 2.12 (s, 0.8H, OH), 3.60–4.65 (m, 13H, H², H³, H⁴, H⁵, H⁶, H⁶, CH₂^{Fmoc}, CH^{Fmoc}, H₂O), 5.47 (brs, 1H, H⁸), 5.80 (brs, 1H, H¹), 7.32 (m, 2H, H^{arom}), 7.40 (m, 2H, H^{arom}), 7.57 (m, 2H, H^{arom}), 7.76 (d, *J* = 6.7 Hz, 2H, H^{arom}); ¹³C NMR (125 MHz, CDCl₃, 300 K): δ = 26.46 (CH₃), 26.61 (CH₃), 47.12 (CH^{Fmoc}), 55.74 (C³), 63.73 (C⁴), 67.47 (C⁵), 79.25 (C²), 80.41 (CH₂^{Fmoc}), 103.77 (C¹), 112.85 (C^{isoprop}), 120.05 (C^{arom}), 124.90 (C^{arom}), 127.80 (C^{arom}), 141.32, 143.53, 143.57 (C^{arom}, C⁶); ESI-MS: calcd for C₂₂H₂₂NO₇Na: 464.1685; found: 464.1; *t*_R = 14.41 min (HPLC-MS, 30–90% B in 20 min).

3-Amino-3-deoxy-*N*-9-fluorenylmethoxycarbonyl-1,2-isopropylidene-α-D-allofuranic acid (f-SAA2): Diol **10** and TEMPO (1 mg, 0.064 mmol, 0.011 equiv) were suspended in CH₂Cl₂ (1.8 mL) at 0 °C, a solution of KBr (14.5 mg, 0.064 mmol, 0.11 equiv) and *t*Bu₄NCl (8.9 mg) in sat. aq NaHCO₃ (1.2 mL) was added slowly. To this a mixture of NaOCl (13%, 1.5 mL), sat. aq NaCl (1.32 mL) and sat. aq NaHCO₃ (0.7 mL) were added dropwise over a period of 30 min. The reaction mixture was stirred overnight, diluted with AcOEt (2 mL). The organic phase was extracted twice with brine. The aq phase was adjusted to pH 2 with diluted HCl (1 N) and extracted with AcOEt. Removal of the combined organic phases under reduced pressure afforded **2** as a colorless syrup (0.17 g, 62%). ¹H NMR (500 MHz, [D₆]DMSO, 300 K): δ = 1.25 (s, 3H, CH₃), 1.47 (s, 3H, CH₃), 4.05–4.30 (m, 6H, H³, H⁴, H⁵, CH₂^{Fmoc}, CH^{Fmoc}), 4.55 (brs, 1H, H²), 5.73 (brs, 1H, H¹), 7.30–7.90 (m, 9H, H^{arom}, H^N); ¹³C NMR (125 MHz, [D₆]DMSO, 300 K): δ = 23.97 (CH₃), 24.39 (CH₃), 45.19 (CH^{Fmoc}), 51.88 (C³), 63.70 (C⁴), 67.18 (C⁵), 75.30 (C²), 76.98 (CH₂^{Fmoc}), 101.73 (C¹), 111.35 (C^{isoprop}), 117.20 (C^{arom}), 122.39 (C^{arom}), 124.14 (C^{arom}), 124.51 (C^{arom}), 143.80 (C⁶); FAB-HRMS calcd for C₂₄H₂₅NO₈Na: 478.1478; found: 478.14167 [*M*+Na]⁺; *t*_R = 15.71 (HPLC-MS, 10–90% B in 20 min).

Fmoc-[fSAA1-β-hGly]₃-OH (3): In a syringe (10 mL), equipped with a frit, preloaded H-β-hGly-2-ClTrr resin (399.5 mg, 0.44 mmol g^{–1}, 0.17578 mmol) was swelled for 45 min in NMP. According to GP 2, Fmoc-f-SAA1-OH (0.1494 g, 0.35156 mmol, 2 equiv) and Fmoc-β-hGly-OH (0.1642 g, 0.5273 mmol, 3 equiv) were coupled alternately to yield the hexamer. The linear peptide was cleaved off the resin to yield crude **3** as a redish syrup, which was purified by RP-HPLC (40.5–54% B in 30 min) to yield the title compound (71.3 mg, 41%) as a white, fluffy solid. ¹H NMR (600 MHz, [D₆]DMSO, 296 K): δ = 1.223 (fSAA1, CH₃), 1.242 (fSAA1, CH₃), 1.264 (fSAA1, CH₃), 1.279 (fSAA1, CH₃), 1.386 (fSAA1³, CH₃), 1.413 (fSAA1, CH₃), 2.220 (β-hGly⁴, H^a), 2.263 (β-hGly², H^a), 2.304 (β-hGly⁴,

H^α), 2.318 (β-hGly², H^α), 2.378 (β-hGly⁶, H^α), 3.192 (β-hGly⁴, ³J(H^N,H^β) = 6.1 Hz, H^β), 3.203 (β-hGly², ³J(H^N,H^β) = 5.8 Hz, H^β), 3.204 (β-hGly⁶, ³J(H^N,H^β) = 5.7 Hz, H^β), 3.298 (β-hGly⁶, ³J(H^N,H^β) = 6.7 Hz, H^β), 3.328 (β-hGly⁴, ³J(H^N,H^β) = 6.4 Hz, H^β), 3.330 (β-hGly², ³J(H^N,H^β) = 6.8 Hz, H^β), 4.020 (fSAA1¹, ³J(H¹,H⁴) = 10.0, ³J(H^N,H³) = 8.9 Hz, H³), 4.066 (fSAA1³, ³J(H³,H⁴) = 10.4 Hz, H⁴), 4.071 (fSAA1⁵, ³J(H³,H⁴) = 10.0 Hz, H⁴), 4.200 (fSAA1¹, ³J(H³,H⁴) = 10.0 Hz, H⁴), 4.219 (CH^{Fmoc}), 4.256 (fSAA1⁵, ³J(H³,H⁴) = 10.0, ³J(H^N,H³) = 8.8 Hz, H³), 4.296 (CH₂^{Fmoc}), 4.335 (fSAA1³, ³J(H³,H⁴) = 10.4, ³J(H^N,H³) = 9.1 Hz, H³), 4.583 (fSAA1¹, ³J(H¹,H²) = 5.3 Hz, H²), 4.565 (fSAA1³, ³J(H¹,H²) = 5.3 Hz, H²), 4.576 (fSAA1⁵, ³J(H¹,H²) = 5.3 Hz, H²), 5.85 (fSAA1, ³J(H¹,H²) = 5.3 Hz, H¹), 7.317 (Fmoc), 7.401 (Fmoc), 7.549 (fSAA1³, ³J(H^N,H³) = 8.9 Hz, H^N), 7.731 (Fmoc), 7.813 (β-hGly⁴, ³J(H^N,H^β) = 6.1, ³J(H^N,H^β) = 6.4 Hz, H^N), 7.837 (β-hGly², ³J(H^N,H^β) = 5.8, ³J(H^N,H^β) = 6.8 Hz, H^N), 7.885 (Fmoc), 7.905 (β-hGly⁶, ³J(H^N,H^β) = 5.7, ³J(H^N,H^β) = 6.7 Hz, H^N), 8.050 (fSAA1⁵, ³J(H^N,H³) = 8.8 Hz, H^N), 8.098 (fSAA1³, ³J(H^N,H³) = 9.1 Hz, H^N), 12.212 (β-hGly⁶, COOH); temperature coefficients [−Δδ/ΔT]: ¹H NMR (500 MHz, CD₃CN, 295–320 K, ΔT = 5 K) f-SAA1¹/H^N: 4.92; β-hGly²/H^N: 2.48; f-SAA1³/H^N: 7.90; β-hGly⁴/H^N: 4.17; f-SAA1⁵/H^N: 9.25; β-hGly⁶/H^N: 1.95; ¹³C NMR (150 MHz, [D₆]DMSO, 296 K): δ = 22.179 (fSAA1, CH₃), 23.012 (fSAA1¹⁻³, CH₃), 26.207 (fSAA1, CH₃), 26.393 (fSAA1, CH₃), 28.708 (fSAA1, CH₃), 29.588 (fSAA1, CH₃), 33.266 (β-hGly⁶, C^α), 34.6 (β-hGly, C^β), 34.7 (β-hGly²⁺⁴, C^α), 35.2 (β-hGly, C^β), 46.383 (Fmoc, CH), 54.388 (fSAA1⁵, C³), 54.560 (fSAA1³, C³), 56.726 (fSAA1¹, C³), 65.662 (Fmoc, CH₂), 76.360 (fSAA1¹, C⁴), 76.660 (fSAA1³⁺⁵, C⁴), 78.575 (fSAA1, C²), 104.103 (fSAA1, C¹), 119.871 (Fmoc, CH^{arom}), 125.04 (Fmoc, CH^{arom}), 126.967 (Fmoc, CH^{arom}), 127.226 (Fmoc, CH^{arom}), 155.429 (Fmoc, NCOO), 168.149 (fSAA1¹, C⁵), 168.297 (fSAA1⁵, C⁵), 168.515 (fSAA1³, C⁵), 170.431 (β-hGly⁴, CO), 170.590 (β-hGly², CO); ¹⁵N NMR (60 MHz, [D₆]DMSO, 296 K): δ = 78.46 (fSAA1¹, NH), 110.86 (β-hGly⁴, NH), 111.53 (fSAA1⁵, NH), 111.84 (β-hGly⁶, NH), 118.25 (fSAA1³, NH), 111.88 (β-hGly², NH); *t*_R = 13.65 (HPLC-ESI-MS, 30–90% B in 20 min); ESI-MS: 1053.2 [M–H+2Na]⁺, 1047.2 [M+K]⁺, 1031.3 [M+Na]⁺, 1009.1 [M+H]⁺; FAB-HRMS: calcd for C₄₈H₆₀N₆O₁₈Na: 1031.3861; found: 1031.3852 [M+Na]⁺.

Fmoc-[f-SAA2-GABA]₃-OH (4): In a syringe (10 mL), equipped with a frit, TCP resin (1.0550 g, ≈0.95 mmol g^{−1}) was swelled in NMP (30 min). After filtering off the resin, a solution of Fmoc-GABA-OH (0.3274 g, 1.002 mmol, 1 equiv) and (iPr)₂EtN (0.51 mL, 3.004 mmol, 3 equiv) in CH₂Cl₂ (7.5 mL) was added. After 2 h the resin was filtered off, washed with CH₂Cl₂ (3 × 3 min), DMF (3 × 3 min) and MeOH (3 × 3 min) before dried under reduced pressure overnight. The resin loading was 0.591 mmol g^{−1} according to gravimetric measurements. In a syringe (10 mL) the GABA loaded resin (0.3164 g, 0.591 mmol g^{−1}, 0.187 mmol) was swelled for 30 min in NMP. According to **GP 2** Fmoc-f-SAA2-OH (0.1703 g, 0.3798 mmol, 2 equiv) and Fmoc-GABA (0.1825 g, 0.5610 mmol, 3 equiv) were coupled alternately. Purification by RP-HPLC (36–50% B in 30 min) yielded **4** (10 mg, 4.7%). ¹H NMR (600 MHz, [D₃]pyridine, 300 K): δ = 1.181 (fSAA2³, CH₃), 1.195 (fSAA2³, CH₃), 1.199 (fSAA2⁵, CH₃), 1.218 (fSAA2⁵, CH₃), 1.243 (fSAA2¹, CH₃), 1.301 (fSAA2¹, CH₃), 2.097 (GABA⁶, H^β), 2.113 (GABA⁴, H^β), 2.127 (GABA², H^β), 2.499 (GABA², H^α), 2.592 (GABA⁴, H^α), 2.607 (GABA⁶, H^α), 3.414 (GABA⁴, H^γ), 3.431 (GABA², H^γ), 3.525 (GABA⁶, H^γ), 3.686 (GABA²⁺⁴, H^γ), 3.728 (GABA⁶, H^γ), 4.035 (Fmoc, CH), 4.272 (Fmoc, CH₂), 4.715 (fSAA2³, H³), 4.774 (fSAA2⁵, H³), 4.833 (fSAA2¹, H²), 4.992 (fSAA2¹, H⁵), 4.998 (fSAA2³, H⁴), 4.999 (fSAA2³, H⁵), 5.018 (fSAA2⁵, H⁵), 5.031 (fSAA2⁵, H⁴), 5.100 (d, *J* = 10.1 Hz, fSAA2¹, H⁴), 5.233 (fSAA2¹, H³), 5.391 (fSAA2³, H³), 5.47 (fSAA2⁵, H³), 5.897 (d, *J* = 2.6 Hz, fSAA2³, H¹), 5.938 (d, *J* = 2.5 Hz, fSAA2⁵, H¹), 5.985 (brs, fSAA2¹, H¹), 7.223 (m, Fmoc, H^{arom}), 7.359 (m, Fmoc, H^{arom}), 7.658 (m, Fmoc, H^{arom}), 7.806 (t, *J* = 5.9 Hz, Fmoc, H^{arom}), 8.611 (GABA⁴, H^N), 8.633 (GABA², H^N), 8.69 (GABA⁶, H^N), 9.255 (d, *J* = 9.4 Hz, fSAA2³, H^N), 9.289 (*J* = 9.5 Hz, SAA2¹, H^N), 9.303 (*J* = 9.6 Hz, fSAA2⁵, H^N); ¹³C NMR (150 MHz, [D₃]pyridine, 300 K): δ = 22.94 (fSAA2³, CH₃), 23.6 (fSAA2¹, CH₃), 25.7 (GABA, C^β), 26.14 (fSAA2⁵, CH₃), 30.13 (fSAA2¹, CH₃), 31.78 (fSAA2³, CH₃), 31.91 (GABA⁶, C^α), 33.3 (GABA², C^α), 33.35 (GABA⁴, C^α), 38.49 (GABA⁴, C^γ), 38.7 (GABA², C^γ), 39.15 (GABA⁶, C^γ), 47.196 (Fmoc, CH₂), 50.15 (fSAA2³, C³), 50.3 (fSAA2⁵, C³), 52.5 (fSAA2¹, C³), 61.139 (Fmoc, CH), 70.4 (fSAA2, C⁵), 80 (fSAA2¹⁺⁵, C⁵), 80.1 (fSAA2³, C⁵), 81 (fSAA2, C⁴), 104.3 (fSAA2³⁺⁵, C¹), 104.4 (fSAA2¹, C¹), 111 (fSAA2, C^{isoprop}), 119.917 (Fmoc, C^{arom}), 125.410 (Fmoc, C^{arom}), 127.063 (Fmoc, C^{arom}), 127.647 (Fmoc, C^{arom}), 171.3 (fSAA2, CO), 173 (GABA², CO), 173.2 (GABA⁴⁺⁶, CO); *t*_R = 17.06 min (30–60% B in

30 min); ESI-MS: 1185 [M–H+2Na]⁺, [M–H+2K]⁺, 1179.2 [M+K]⁺, 1163.4 [M+Na]⁺, 1141.1 [M+H]⁺, 1083.1, 1025.1, 967.1, 179.1; HRMS: *m/z*: calcd for C₃₄H₇₃N₆O₂₁: 1141.482884; found: 1141.4829 [M+H]⁺.

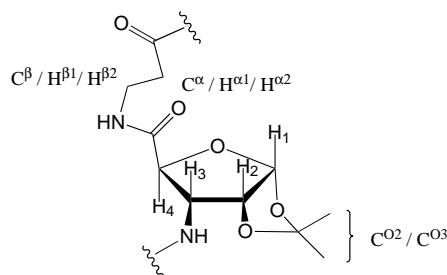
cyclo-[f-SAA1-β-hGly]₃ (5): Peptide **3** (8.9 mg) was dissolved in 20% piperidine in DMF (300 μL). After 30 min deprotection was complete. Purification by RP-HPLC (20–80% B in 30 min) afforded deprotected **3** as a white fluffy powder (6.5 mg, quantitative). Compound **3** (3.9 mg, 4.96 × 10^{−3} mmol) was dissolved in DMF (11 mL), a solution of HATU (1 mL of a solution of 18.8 mg HATU in 10 mL DMF) and 2,4,6-collidine (6.5 μL) were added. After 24 h reaction was not complete. Additional HATU solution (100 μL of a solution of 18.8 mg HATU in 10 mL DMF) and 2,4,6-collidine (1 μL) were added. After further 2 h the reaction was complete (HPLC control). Purification by RP-HPLC (20–80% B in 30 min) afforded **5** as a white fluffy solid (3.8 mg, quant.). ¹H NMR (500 MHz, [D₆]DMSO, 300 K): δ = 1.29 (s, 9H, 3 × CH₃), 1.46 (s, 9H, 3 × CH₃), 2.18 (m, 3H, 3 × H^α), 2.29 (m, 3H, 3 × H^α), 3.19 (m, 3H, 3 × H^β), 3.42 (m, 3H, 3 × H^β), 4.20 (m, 6H, 3 × H³ + 3 × H⁴), 4.64 (dd, *J*(H²,H¹) = 3.26, *J*(H²,H³) = 4.24, 3H, 3 × H²), 5.82 (d, *J* = 3.3 Hz, 3H, 3 × H¹), 7.67 (t, *J* = 6.0 Hz, 3 × β-hGly-H^N), 8.03 (d, *J* = 7.0 Hz, 3 × fSAA1-H^N); ¹³C NMR (125 MHz, [D₆]DMSO, 300 K, HMQC experiment): δ = 26.23 (CH₃), 26.46 (CH₃), 35.13 (C^β), 35.37 (C^α), 54.83 (C³), 76.63 (C⁴), 78.98 (C²), 104.05 (C¹); *t*_R = 20 min (15–85% B in 30 min); ESI-MS: 921.3 [M+TFA+K]⁺, 905.3 [M+TFA+Na]⁺, 807.4 [M+K]⁺, 791.5 [M+Na]⁺, 769.3 [M+H]⁺.

NMR and structure determination of 3 in CD₃CN: (the measurements in [D₆]DMSO are not described in this section and were not used for deducing the 12/10/12 helical structure): All NMR spectra were acquired at 300 K in CD₃CN on a Bruker DMX500 spectrometer, processed and analyzed using the X-WINNMR [X-WINNMR V3.0, Bruker, Karlsruhe] and AURELIA [AURELIA V2.8.11, Bruker, Karlsruhe] software, respectively. As described previously, sequential assignment was done using information on the intrareidual and sequential C^β, C^γ, H^α and H^N chemical shifts taken from COSY,^[46] TOCSY,^[45] HMQC^[47] and HMBC^[48] experiments. The COSY, HMQC and HMBC were all recorded with 8192 (*t*₂) × 512 (*t*₁) complex points using 8, 16 and 64 scans per increment, respectively. A mixing time of 75 ms and a data size of 2048 × 512 in *t*₂ and *t*₁, respectively, were used for the TOCSY experiment. NOESY^[49] experiments using four mixing times (100, 200, 400, 600 ms) were measured and distance data were derived from the NOESY spectra (8192 (*t*₂) × 512 (*t*₁) complex points and 16 scans per increment). A mixing time of 400 ms was necessary to achieve adequate cross-peak intensities. At this mixing time, most of the NOE build up curves were still in the linear region. However, some of the integrated 76 NOESY cross-peaks were adjusted manually to account for spin diffusion. On the derived distances, a tolerance of ±10% was applied to obtain upper and lower bound distance restraints for structural calculations. Allowances for the use of pseudo-atoms were added only for the terminal H^α and H^β spin groups of β-hGly⁶, which could not be assigned stereospecifically. All 76 NOEs used for structural calculations are listed in Table 2.

A first restrained conformational search was performed with the X-PLOR package,^[50] using standard simulated annealing protocols, yielding an ensemble of 10 structures with good convergence. This ensemble already clearly showed a 12/10/12 helical conformation. The structure which best fulfilled the experimental restraints was then used as a starting structure for a 150 ps simulated dynamics run in the CVFF forcefield, using Discover V2.98.^[51] Since to our knowledge no explicit, all-atom acetonitrile solvent box is available for this program package, we equilibrated a solvent box of 31.3 × 31.9 × 31.5 Å³ containing 360 CH₃CN molecules for this purpose. The dynamics run was then performed in a solvent box of 47 × 47 × 47 Å³ containing 1039 CH₃CN molecules, and using the equilibrated box as a template. During simulation time, 1500 frames were collected in the trajectory. Restraint violations all remained below 0.1 Å, except for one contact. Averaging of the heavy atom coordinates over the 150 ps trajectory, and subsequent 300 steps of steepest descent minimization yielded the structure of **3**, as described in the main section. Trajectory population statistics for the hydrogen bonds are shown in Table 3.

To test the stability of the average minimized structure under unrestrained conditions, it was used as the starting structure for a further free dynamics simulation of 150 ps duration in explicit solvent (CH₃CN Box, dimensions 43 × 43 × 43 Å³, 779 CH₃CN molecules). During this simulation, 5 restraints were violated by more than 0.1 Å. The violated NOEs indicate an occasional, partial unwinding of the helix, which can be explained by the fact that acetonitrile is not a completely unpolar solvent.

Table 2. The 76 NOESY cross-peaks and average distance restraint violations for oligomer **3** in CH₃CN used for the structural calculations.



Residue 1	Atom 1	Residue 2	Atom 2	Lower bound	Upper bound	Calcd distance (r^{-3}_{av})	Calcd distance (r_{av})	$d(r^3)$	$d(r)$
f-SAA1 ¹	H ^N	f-SAA1 ¹	H ²	3.510	4.290	3.465	3.507	− 0.045	− 0.003
f-SAA1 ¹	H ^N	f-SAA1 ¹	H ³	2.700	3.300	3.035	3.039	0.000	0.000
f-SAA1 ¹	H ^N	f-SAA1 ¹	H ⁴	2.700	3.300	2.722	2.760	0.000	0.000
f-SAA1 ¹	H ^N	f-SAA1 ¹	C ^{O2}	3.630	6.100	4.310	4.364	0.000	0.000
f-SAA1 ¹	H ^N	f-SAA1 ¹	C ^{O3}	3.630	6.100	5.117	5.156	0.000	0.000
f-SAA1 ¹	H ¹	f-SAA1 ¹	C ^{O2}	3.630	6.100	4.344	4.347	0.000	0.000
f-SAA1 ¹	H ¹	f-SAA1 ¹	C ^{O3}	2.030	4.100	3.854	3.875	0.000	0.000
f-SAA1 ¹	H ¹	f-SAA1 ³	H ⁴	4.500	5.500	4.540	4.603	0.000	0.000
f-SAA1 ¹	H ²	f-SAA1 ¹	H ³	2.160	2.640	2.348	2.357	0.000	0.000
f-SAA1 ¹	H ²	f-SAA1 ¹	C ^{O2}	3.730	6.200	4.301	4.304	0.000	0.000
f-SAA1 ¹	H ²	f-SAA1 ¹	C ^{O3}	2.130	4.200	3.461	3.482	0.000	0.000
f-SAA1 ¹	H ³	f-SAA1 ³	H ⁴	2.700	3.300	2.646	2.700	− 0.054	0.000
f-SAA1 ¹	H ³	f-SAA1 ³	C ^{O2}	2.830	5.100	4.892	4.983	0.000	0.000
f-SAA1 ¹	H ⁴	f-SAA1 ¹	C ^{O2}	2.130	4.200	3.421	3.461	0.000	0.000
β -hGly ²	H ^N	β -hGly ²	H ^{<i>a2</i>}	2.900	3.500	3.455	3.476	0.000	0.000
β -hGly ²	H ^N	β -hGly ²	H ^{<i>\beta</i>1}	2.700	3.300	3.028	3.033	0.000	0.000
β -hGly ²	H ^N	β -hGly ²	H ^{<i>\beta</i>2}	2.250	2.750	2.472	2.482	0.000	0.000
β -hGly ²	H ^N	f-SAA1 ¹	H ⁴	3.200	4.000	3.496	3.504	0.000	0.000
β -hGly ²	H ^N	f-SAA1 ³	H ⁴	4.000	5.000	4.095	4.177	0.000	0.000
β -hGly ²	H ^{<i>a1</i>}	β -hGly ²	H ^{<i>\beta</i>1}	2.250	2.750	2.437	2.445	0.000	0.000
β -hGly ²	H ^{<i>a1</i>}	β -hGly ²	H ^{<i>\beta</i>2}	2.250	2.750	2.512	2.522	0.000	0.000
β -hGly ²	H ^{<i>a1</i>}	f-SAA1 ⁵	C ^{O2}	3.630	6.100	4.030	4.197	0.000	0.000
β -hGly ²	H ^{<i>a2</i>}	β -hGly ²	H ^{<i>\beta</i>1}	2.250	2.750	2.517	2.527	0.000	0.000
β -hGly ²	H ^{<i>a2</i>}	β -hGly ²	H ^{<i>\beta</i>2}	2.700	3.300	3.087	3.090	0.000	0.000
f-SAA1 ³	H ^N	f-SAA1 ¹	H ³	2.700	3.300	3.141	3.227	0.000	0.000
f-SAA1 ³	H ^N	β -hGly ²	H ^{<i>a2</i>}	2.250	2.750	2.159	2.174	− 0.091	− 0.076
f-SAA1 ³	H ^N	f-SAA1 ³	H ²	3.200	4.000	3.474	3.495	0.000	0.000
f-SAA1 ³	H ^N	f-SAA1 ³	H ³	2.700	3.300	3.068	3.070	0.000	0.000
f-SAA1 ³	H ^N	f-SAA1 ³	H ⁴	2.700	3.300	2.682	2.706	− 0.018	0.006
f-SAA1 ³	H ^N	f-SAA1 ³	C ^{O2}	2.630	5.100	4.217	4.256	0.000	0.000
f-SAA1 ³	H ¹	f-SAA1 ³	H ²	2.430	2.970	2.364	2.373	− 0.066	− 0.057
f-SAA1 ³	H ¹	f-SAA1 ³	H ³	3.060	3.740	3.047	3.065	− 0.013	0.005
f-SAA1 ³	H ¹	f-SAA1 ³	C ^{O3}	2.230	4.300	3.853	3.871	0.000	0.000</

Table 2 (cont.)

Residue 1	Atom 1	Residue 2	Atom 2	Lower bound	Upper bound	Calcd distance (r^{-3}_{av})	Calcd distance (r_{av})	$d(r^3)$	$d(r)$
f-SAA1 ⁵	H ^N	f-SAA ³	H ³	2.250	2.750	2.746	2.802	0.000	0.052
f-SAA1 ⁵	H ^N	β -hGly ⁴	H ^{α1}	3.150	3.850	3.335	3.345	0.000	0.000
f-SAA1 ⁵	H ^N	β -hGly ⁴	H ^{α2}	2.250	2.750	2.189	2.205	−0.061	−0.045
f-SAA1 ⁵	H ^N	f-SAA1 ⁵	H ²	3.200	4.000	3.562	3.582	0.000	0.000
f-SAA1 ⁵	H ^N	f-SAA1 ⁵	H ³	2.700	3.300	3.072	3.075	0.000	0.000
f-SAA1 ⁵	H ^N	f-SAA1 ⁵	H ⁴	2.610	3.190	2.636	2.657	0.000	0.000
f-SAA1 ⁵	H ^N	f-SAA1 ⁵	C ^{O2}	3.630	6.100	4.171	4.205	0.000	0.000
f-SAA1 ⁵	H ¹	f-SAA1 ⁵	H ³	2.880	3.520	3.101	3.120	0.000	0.000
f-SAA1 ⁵	H ¹	f-SAA1 ⁵	H ⁴	3.510	4.290	3.798	3.802	0.000	0.000
f-SAA1 ⁵	H ¹	f-SAA1 ⁵	C ^{O2}	3.630	6.100	4.350	4.352	0.000	0.000
f-SAA1 ⁵	H ¹	f-SAA1 ⁵	C ^{O3}	1.930	4.000	3.802	3.822	0.000	0.000
f-SAA1 ⁵	H ²	f-SAA1 ⁵	H ⁴	3.420	4.180	3.823	3.828	0.000	0.000
f-SAA1 ⁵	H ²	f-SAA1 ⁵	C ^{O2}	3.630	6.100	4.319	4.322	0.000	0.000
f-SAA1 ⁵	H ²	f-SAA1 ⁵	C ^{O3}	2.130	4.200	3.523	3.540	0.000	0.000
f-SAA1 ⁵	H ⁴	f-SAA1 ⁵	C ^{O2}	1.930	4.000	3.250	3.276	0.000	0.000
f-SAA1 ⁵	H ⁴	f-SAA1 ⁵	C ^{O3}	2.930	5.200	4.816	4.825	0.000	0.000
β -hGly ⁶	H ^N	f-SAA1 ⁵	H ¹	3.150	3.850	3.716	3.748	0.000	0.000
β -hGly ⁶	H ^N	f-SAA1 ⁵	H ³	3.200	4.000	2.892	2.967	−0.308	−0.233
β -hGly ⁶	H ^N	f-SAA1 ⁵	H ⁴	3.200	4.000	3.444	3.456	0.000	0.000
β -hGly ⁶	H ^N	β -hGly ⁶	C ^{α}	2.830	5.000	2.895	2.922	0.000	0.000
β -hGly ⁶	H ^N	β -hGly ⁶	C ^{β}	2.130	4.100	2.212	2.214	0.000	0.000

Table 3. Trajectory population statistics for hydrogen bonds.

Acceptor–Donor Pair	Average N–O distance [Å]	Average H–O distance [Å]	Average N–H–O angle [°]	Population [%]
Fmoc CO–f-SAA1 ³ HN	3.77	2.94	142.5	52.2
f-SAA1 ³ CO– β -hGly ² HN	3.70	2.86	142.6	41.0
β -hGly ² CO–f-SAA1 ³ HN	3.30	2.34	158.0	85.5
fSAA1 ⁵ CO– β -hGly ⁴ HN	3.52	2.62	149.9	65.5

Acknowledgements

The authors thank B. Cordes, M. Goede, M. Kranawetter, the graduate student T. Poethko, Dr. W. Spahl, and M. Wolff for technical assistance. Financial support by the Fonds der Chemischen Industrie is gratefully acknowledged.

- [1] D. H. Appella, L. A. Christianson, I. L. Karle, D. R. Powell, S. H. Gellman, *J. Am. Chem. Soc.* **1996**, *118*, 13071–13072.
- [2] E. Graf von Roedern, H. Kessler, *Angew. Chem.* **1994**, *106*, 684–686; *Angew. Chem. Int. Ed. Engl.* **1994**, *33*, 667–669.
- [3] E. Graf von Roedern, E. Lohof, G. Hessler, M. Hoffmann, H. Kessler, *J. Am. Chem. Soc.* **1996**, *118*, 10156–10167.
- [4] Y. Suhara, J. E. K. Hildreth, Y. Ichikawa, *Tetrahedron Lett.* **1996**, *37*, 1575–1578.
- [5] Y. Suhara, M. Ichikawa, J. E. K. Hildreth, Y. Ichikawa, *Tetrahedron Lett.* **1996**, *37*, 2549–2552.
- [6] L. Szabo, B. L. Smith, K. D. McReynolds, A. L. Parrill, E. R. Morris, J. Gervay, *J. Org. Chem.* **1998**, *63*, 1074–1078.
- [7] E. Lohof, F. Burkhart, M. A. Born, E. Planker, H. Kessler, *Adv. Amino Acid Mimetics Peptidomimetics*, **1999**, 2 263–292.
- [8] D. E. A. Brittain, M. P. Watterson, T. D. W. Claridge, M. D. Smith, G. W. J. Fleet, *J. Chem. Soc. Perkin Trans. 1* **2000**, 3655–3665.
- [9] N. L. Hungerford, T. D. W. Claridge, M. P. Watterson, R. T. Aplin, A. Moreno, G. W. J. Fleet, *J. Chem. Soc. Perkin Trans. 1* **2000**, 3666–3679.
- [10] E. Lohof, M. A. Born, H. Kessler, in *Synthesis of Peptides and Peptidomimetics*, Vol. E22b (Eds.: M. Goodman, A. Felix, L. Moroder, C. Toniolo), Georg Thieme Verlag, Stuttgart, in press.
- [11] S. A. W. Gruner, E. Locardi, E. Lohof, H. Kessler, *Chem. Rev.* **2002**, *102*, 491–514.
- [12] K. Heyns, H. Paulsen, *Chem. Ber.* **1955**, *108*, 188–195.
- [13] E.-F. Fuchs, J. Lehmann, *Chem. Ber.* **1975**, *108*, 2254–2260.
- [14] R. P. Cheng, S. H. Gellman, W. F. DeGrado, *Chem. Rev.* **2001**, *101*, 3219–3232.
- [15] D. Seebach, M. Overhand, F. N. M. Kühnle, B. Martinoni, L. Oberer, U. Hommel, H. Widmer, *Helv. Chim. Acta* **1996**, *79*, 913–941.
- [16] K. Gademann, D. Seebach, *Helv. Chim. Acta* **1999**, *82*, 957–962.
- [17] D. Seebach, S. Abele, T. Sifferlen, M. Hänggi, S. Gruner, P. Seiler, *Helv. Chim. Acta* **1998**, *81*, 2218–2243.
- [18] T. Hintermann, K. Gademann, B. Jaun, D. Seebach, *Helv. Chim. Acta* **1998**, *81*, 983–1002.
- [19] D. H. Appella, L. A. Christianson, D. A. Klein, D. R. Powell, X. Huang, J. J. Barchi Jr., S. H. Gellman, *Nature* **1997**, *38*, 381–384.
- [20] S. Krauthäuser, L. A. Christianson, D. R. Powell, S. H. Gellman, *J. Am. Chem. Soc.* **1997**, *119*, 11719–11720.
- [21] H. E. Stanger, S. H. Gellman, *J. Am. Chem. Soc.* **1998**, *120*, 4236–4237.
- [22] X. Wang, J. F. Espinosa, S. H. Gellman, *J. Am. Chem. Soc.* **2000**, *122*, 4821–4822.
- [23] M. Brenner, D. Seebach, *Helv. Chim. Acta* **2001**, *84*, 1181–1189.
- [24] M. G. Woll, J. R. Lai, I. A. Guzei, S. J. C. Taylor, M. E. B. Smith, S. H. Gellman, *J. Am. Chem. Soc.* **2001**, *123*, 11077–11078.
- [25] D. Seebach, K. Gademann, J. V. Schreiber, J. L. Matthews, T. Hintermann, B. Jaun, *Helv. Chim. Acta* **1997**, *80*, 2033–2038.
- [26] K. A. Bode, J. Applequist, *Macromolecules* **1997**, *30*, 2144–2150.
- [27] J. Applequist, K. A. Bode, D. H. Appella, L. A. Christianson, S. H. Gellman, *J. Am. Chem. Soc.* **1998**, *120*, 4891–4892.
- [28] H. L. Schenck, S. H. Gellman, *J. Am. Chem. Soc.* **1998**, *120*, 4869–4870.

- [29] Y. Suhara, M. Izumi, M. Ichikawa, M. B. Penno, Y. Ichikawa, *Tetrahedron Lett.* **1997**, 38, 7167–7170.
- [30] M. Stöckle, E. Locardi, S. Gruner, H. Kessler, in *20th International Carbohydrate Symposium* (Ed.: J. Thiem), LCI Publisher GmbH, Hamburg, **2000**, p. 124.
- [31] R. M. van Well, H. S. Overkleeft, M. Overhand, E. Vang Carstensen, G. A. van der Marel, J. H. van Boom, *Tetrahedron Lett.* **2000**, 41, 9331–9335.
- [32] S. Gruner, E. Locardi, M. Stöckle, H. Kessler, in *20th International Carbohydrate Symposium* (Ed.: J. Thiem), LCI Publisher, Hamburg, Germany, **2000**, B132.
- [33] S. Gruner, H. Kessler, in *26th European Peptide Symposium* (Eds.: J. Martinez, J.-A. Fehrentz), Editions Medicales et Scientifiques, Montpellier, France, **2000**, pp. 313–314.
- [34] M. A. Ondetti, J. Pluscec, E. R. Weaver, N. Williams, E. F. Sabo, O. Kocy, in *3rd Am. Pept. Symp.* (Ed.: J. Meienhofer), Ann Arbor Sci., Ann Arbor, Mich, **1972**, pp. 525–531.
- [35] T. Hintermann, D. Seebach, *Synlett* **1997**, 5, 437–438.
- [36] S. A. W. Gruner, G. Kéri, R. Schwab, A. Venetianer, H. Kessler, *Org. Lett.* **2001**, 3, 3723–3725.
- [37] L. Daley, C. Monneret, C. Gautier, P. Roger, *Tetrahedron Lett.* **1992**, 33, 3749–3752.
- [38] J. M. G. Fernández, C. O. Mellet, J. L. J. Blanco, J. Fuentes, *J. Org. Chem.* **1994**, 59, 5565–5572.
- [39] H. H. Baer, Y. Gan, *Carbohydr. Res.* **1991**, 210, 233–245.
- [40] L. N. Kulinkovich, V. A. Timoshchuk, *J. Gen. Chem. USSR (Engl. Transl.)* **1983**, 53, 1917–1922.
- [41] G. B. Fields, R. L. Nobel, *Int. J. Pept. Protein Res.* **1990**, 35, 161–214.
- [42] L. A. Carpino, A. El-Faham, F. Albericio, *Tetrahedron Lett.* **1994**, 35, 2279–2282.
- [43] L. A. Carpino, A. El-Faham, C. A. Minor, F. Albericio, *J. Chem. Soc. Chem. Commun.* **1994**, 201–203.
- [44] R. Bollhagen, M. Schmiedberger, K. Barlos, E. Grell, *J. Chem. Soc. Chem. Commun.* **1994**, 2559–2560.
- [45] L. Braunschweiler, R. R. Ernst, *J. Magn. Reson.* **1983**, 53, 521–528.
- [46] W. P. Aue, E. Bartholdi, R. R. Ernst, *J. Chem. Phys.* **1976**, 64, 2229–2246.
- [47] L. Müller, *J. Am. Chem. Soc.* **1979**, 101, 4481–4484.
- [48] A. Bax, M. J. Summers, *J. Am. Chem. Soc.* **1986**, 108, 2093–2094.
- [49] J. Jeener, B. H. Meyer, P. Bachman, R. R. Ernst, *J. Chem. Phys.* **1979**, 71, 4546–4553.
- [50] A. T. Brünger, in *X-PLOR*, 3.851 ed., Yale University Press, New Haven, CT, **1992**.
- [51] Discover, Version 2.98, Biosym Molecular Simulations, San Diego, CA, **1995**.
- [52] K. Möhle, R. Günther, M. Thormann, N. Sewald, H.-J. Hofmann, *Biopolymers* **1999**, 50, 167–184.
- [53] R. Günther, H.-J. Hofmann, K. Kuczera, *J. Phys. Chem. B* **2001**, 105, 5559–5567.
- [54] R. Günther, PhD thesis, University of Leipzig (Germany), **2001**.
- [55] D. Seebach, S. Abele, K. Gademann, G. Guichard, T. Hintermann, B. Jaun, J. L. Matthews, J. V. Schreiber, L. Oberer, U. Hommel, H. Widmer, *Helv. Chim. Acta* **1998**, 81, 932–982.
- [56] C. A. G. Haasnoot, F. A. A. M. de Leeuw, H. P. M. de Leeuw, C. Altona, *Org. Mag. Reson.* **1981**, 15, 43–52.
- [57] D. Seebach, P. E. Ciceri, M. Overhand, B. Jaun, D. Rigo, *Helv. Chim. Acta* **1996**, 79, 2043–2066.
- [58] D. Seebach, J. L. Matthews, *Chem. Commun.* **1997**, 2015–2022.
- [59] J. L. Matthews, M. Overhand, F. N. M. Kühnle, P. E. Ciceri, D. Seebach, *Liebigs Ann. Chem.* **1997**, 1371–1379.
- [60] E. Locardi, M. Stöckle, S. Gruner, H. Kessler, *J. Am. Chem. Soc.* **2001**, 123, 8189–8196.
- [61] L. D. Hall, D. C. Miller, *Carbohydr. Res.* **1976**, 47, 299–305.
- [62] R. W. Binkley, M. G. Ambrose, D. G. Hehemann, *J. Org. Chem.* **1980**, 45, 4387–4391.
- [63] A. Gomtsyan, I. Savelyeva, S. Belyakov, I. Kalvinsh, *Carbohydr. Res.* **1992**, 232, 341–348.

Received: November 28, 2001

Revised: April 23, 2002 [F 3710]